(n,3s) Rydberg spectra of diethyl ether, diisopropyl ether, and methyl vinyl ether: Analysis of the torsional motion

Q. Y. Shang, P. O. Moreno, R. Disselkamp, and E. R. Bernstein

(n,3s) Rydberg spectra of diethyl ether, diisopropyl ether, and methyl vinyl ether: Analysis of the torsional motion

Q. Y. Shang, P. O. Moreno, R. Disselkamp, and E. R. Bernstein
Department of Chemistry, Colorado State University, Fort Collins, Colorado 80523

Two-photon resonance mass resolved excitation spectra are obtained for diethyl ether-h_{10}, diethyl ether-d_{10}, diisopropyl either, and methyl vinyl ether cooled in a supersonic jet expansion. The spectra are assigned as due to $2p3s \leftarrow (2p)^2$ Rydberg excitations: significant progressions in a low energy vibrational mode are observed for both diethyl and diisopropyl ethers, but not for methyl vinyl ether. The transition energies for the vibronic progressions are modeled by a double well potential function of polynomial form truncated at the quartic term. The transition intensities for the progressions are calculated based on a Franck–Condon analysis of the excited state potential surface and a harmonic ground state surface. Calculations identify the progression forming mode as the antigeared torsion of the C–O–C–C dihedral angles. Excitation of diethyl ether from its ground electronic state to its $2p3s$ Rydberg state leads to changes in the dihedral angles (τ_1, τ_2) from $\pm 180°$ to $\pm 157°$. Similar electronic excitation of diisopropyl ether yields changes in (τ_1,τ_2) from $\pm 157°$ in the ground state to $\pm 146°$ in the Rydberg state. The torsional displacement active in the $2p3s \leftarrow (2p)^2$ oxygen Rydberg transition is suggested to arise from the interaction between the diffuse $3s$ electron and the β-methyl groups on both diethyl and diisopropyl ethers.

I. INTRODUCTION

Our understanding of molecular Rydberg states is much less complete than that of molecular valence states. Often one cannot predict whether a Rydberg state or series will be identifiable for a given system. This absence of resolvable Rydberg spectra for a molecule can be attributed to selection rules, weak transition cross sections ($\propto 1/n^3$, n=principal quantum number), and mixing with valence states.[1] Rydberg states can be identified spectroscopically through: their high energy (typically greater than 50 000 cm^{-1}); through narrow linewidths even for higher Rydberg states; transition energies which fit the modified hydrogen atom formula

$$h\nu = \text{I.P.} - \frac{R}{(n-\delta)^2},$$

in which I.P. is the ionization potential toward which the Rydberg series converges, n is the principal quantum number, δ is the quantum defect, and R is the Rydberg constant; and spectral broadening as the sample density or background gas pressure increases.[1]

The best understood example of the effect of a Rydberg excitation on molecular geometry is that of ammonia.[2] In the ground state of ammonia, the lone-pair $2p$ electrons dictate that the molecular geometry is pyramidal. When a $2p$ electron is promoted to the $3s$ excited Rydberg state of ammonia (the first excited singlet state), the molecule adopts a planar conformation. In oxo compounds, such as cyclic ethers, however, the geometry change is much less pronounced upon $3s \leftarrow n$ ($2p$) excitation. Steric interactions with the lone pair $2p$ electrons in ROR molecules cause these systems to remain nonlinear—excitation to the (n,3s) Rydberg state changes the COC angle only slightly,

This point is well demonstrated for 1,4-dioxane and tetrahydropyran.[3]

With the introduction of supersonic jet technology and multiphoton and mass resolved excitation spectroscopy, transitions involving Rydberg states have become much more accessible.[3,4] The approach employs isolated cold molecules or clusters, two photon resonance $(n,3s) \leftarrow (2p)^2$ transitions, additional photons to ionize the Rydberg state, and detection of the excitation through the mass resolved ion current created at a multichannel plate detector. Thus, the higher energy Rydberg excited states can be probed by visible and near ultraviolet light with great sensitivity and mass selectivity. Moreover, two photon spectroscopy can take advantage of new selection rules and polarization techniques.

The molecular Rydberg states of ethers have received considerable attention. The first excited state of ethers is generated by promotion of a $2p$ lone pair electron on oxygen to a $3s$ Rydberg orbital. In water, the simplest molecule of this type, the $3s$ Rydberg state is known to mix strongly with an isoenergetic σ^* valence excited state, leading to dissociation in the first excited state.[1,5-7] Through a series of ether compounds (e.g., water, methanol, dimethyl ether, diethyl ether, diisopropyl ether,etc.), the (n,3s) transition energy decreases as the ether becomes more complex. The Rydberg-valance conjugate state is typically broad and little analysis of it has appeared.[8] Resolved structure has been reported for diethyl ether,[9] which seems to suggest that the increased complexity of the ether alkyl chain lowers the Rydberg $3s$ state transition energy and thereby decouples it from the σ^* valence states. The resolvable vibronic structure also suggests that the Rydberg state is long lived and not dissociative.

In this paper, we report the two photon resonance, one photon ionization, mass resolved excitation spectra for a

series of open chain ethers. Through supersonic jet expansion cooling techniques, the spectra are obtained with high resolution and vibronic patterns can be readily analyzed. The spectra of diethyl and diisopropyl ethers reveal a significant change in molecular geometry upon excitation of these molecules to the $(n,3s)$ excited Rydberg state.

II. PROCEDURES

A. Experiment

The technique of supersonic jet expansion mass resolved excitation spectroscopy, employed to study Rydberg states of isolated molecules and clusters, has already been described.[4] Briefly, the expansion mixture is prepared by vaporizing the sample into an evacuated mixing tank before introducing high pressure helium. The various mixtures made contain 0.1% to 2.0% ether. Expansion nozzle pressure is 50 psig. This pressure gives nearly optimum cooling and high signal intensity. In order to establish that no hot bands are present in the observed spectra and that the samples are indeed cold, a 10% Ar/He mixture is also employed as the expansion gas. The only noticeable effect this mixture has on the spectra is a light (~ 0.3 cm^{-1}) sharpening of the features in the spectra presumably due to enhanced rotational cooling. Diethyl ether, diisopropyl ether, and methyl vinyl ether are purchased from Aldrich Chemical Co. (purity $>98\%$). Diethyl ether-d_{10} (98%) is purchased from Cambridge Isotope Laboratories.

The light source for the multiphoton $(2+1)$ ionization experiment is a Nd^{+3}/YAG pumped laser/dye laser combination. The dye laser fundamental is mixed with the Nd^{+3}/YAG laser fundamental output to achieve the required wavelengths. The dye fundamental output is varied to cover the range 358–410 nm. The dye laser beam is focused on the molecular beam with a 30 cm focal length lens.

Ions resulting from the $2+1$ resonance enhanced ionization are mass resolved with a time-of-flight mass spectrometer. Ion current signals are detected by a microchannel plate detector and processed by a boxcar averager and a 286 computer. Extensive ion fragmentation is observed for these ethers. The reported spectra are confirmed in both fragment and parent mass channels.

B. Calculation

A double well potential energy function is used to simulate the excited state vibrational progression observed for diethyl and diisopropyl ethers. The potential function is represented by a polynomial truncated after the quadratic term as originally proposed by Samorjai and Hornig.[10] The potential can be expressed as

$$V(\xi) = \tfrac{1}{2}\hbar\beta(v_2\xi^2 + v_3\xi^3 + v_4\xi^4) \tag{1}$$

in which ξ is a dimensionless coordinate and is related to the vibrational displacement coordinate x by

$$\xi = \alpha x \tag{2}$$

with

$$\alpha = \left(\frac{\mu\beta}{\hbar}\right)^{1/2}. \tag{3}$$

In Eqs. (1)–(3), μ is the reduced mass, $\hbar$ is Planck's constant divided by 2π, β is an arbitrary frequency, and v_2, v_3, and v_4 are dimensionless adjustable parameters. For a symmetric double well potential (as described here), v_3 is zero and v_2 is negative. Since application of this potential is to a torsional mode, it is expressed in units of mass (distance)^2 and x is expressed in radians.

One can solve the dimensionless Schrödinger equation with this potential by assuming that the trial solution is the sum of harmonic oscillator wave functions $\phi_n(\xi)$,

$$\psi_i(x) = \sum_{n=0}^{N-1} C_{in}\phi_n(\xi), \tag{4}$$

in which N is the size of the basis set. The resulting matrix elements of the secular determinant can be evaluated analytically. The only nonvanishing matrix elements are (in units of $\tfrac{1}{4}\hbar\beta$)[10]

$$H_{n,n} = (2n+1)(1+v_2) + \tfrac{3}{2}(2n^2+2n+1)v_4, \tag{5}$$

$$H_{n,n-1} = \tfrac{3}{2}n(2n)^{1/2}v_3, \tag{6}$$

$$H_{n,n-2} = (v_2-1)[n(n-1)]^{1/2} + (2n-1)[n(n-1)]^{1/2}v_4, \tag{7}$$

$$H_{n,n-3} = [\tfrac{1}{2}n(n-1)(n-2)]^{1/2}v_3, \tag{8}$$

$$H_{n,n-4} = \tfrac{1}{2}[n(n-1)(n-2)(n-3)]^{1/2}v_4. \tag{9}$$

A 50×50 matrix is diagonalized for the calculation. The diagonalization is carried out with a standard FORTRAN routine on an IBM RISC/6000 computer. The eigenvalue solutions are fitted to the observed vibronic frequencies by a least squares method, taking $\tfrac{1}{4}\hbar\beta$, v_2, and v_4 as the adjustable parameters.

The resulting eigenvectors give the wave functions for the vibration. The Franck–Condon factors for the transitions can be evaluated from the square of the overlap integrals between the ground and excited state vibrational wave functions. The ground state vibrational wave functions are approximated as harmonic oscillators, with vibrational frequencies determined from infrared and Raman data, and the excited state wave functions evaluated according to Eq. (4). The vectors C_{in} are obtained as the eigenvectors of the matrix diagonalization. The integration is evaluated numerically.

The deuterium isotope effect on the modes may also be evaluated by this same method. The same potential function form is applied to both the protonated and deuterated molecules. Under this assumption, $\tfrac{1}{4}\hbar\beta$ is kept constant, and v_2 and v_4 are varied according to the reduced mass dependence of the matrix elements

$$v_2^d = \frac{\mu_h}{\mu_d} v_2^h \tag{10}$$
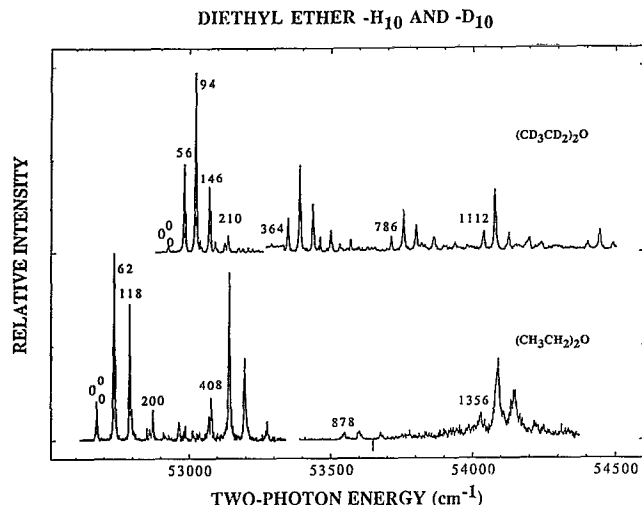
and

DIETHYL ETHER -H₁₀ AND -D₁₀

FIG. 1. Two photon resonance enhanced multiphoton ionization spectra of diethyl ether-h_{10} (bottom trace) and diethyl ether-h_{10} (top trace). The x axis labels represent the two photon transition energies. The 0_0^0 label indicates the spectral origin. The labels on the other spectral features represent their energies in wave numbers relative to the origin (0_0^0).

$$v_4^d = \left(\frac{\mu_h}{\mu_d}\right)^2 v_4^h, \qquad (11)$$

in which μ_h and μ_d are the reduced mass terms for hydrogenated and deuterated molecules, respectively. By making μ_h/μ_d an additional parameter, either known or to be fitted, both sets of isotope data can be modeled simultaneously.

III. RESULTS

A. Diethyl ether

Two photon (2+1) mass resolved excitation spectra (MRES) of diethyl ether-h_{10} and -d_{10} are displayed in Fig. 1. The spectra are obtained by monitoring the ion fragment mass channel with the most intense signal while varying the excitation laser wavelength. The presented spectra cover over 1500 cm^{-1} to the blue of the electronic origin. Due to the dye laser intensity variation with wavelength and the necessity to use a number of dyes to cover this wavelength range, the relative intensities shown in the spectra may not accurately reflect the true vibronic relative intensities of the observed transitions. No attempt is made to correct spectral intensities for the dye laser intensity variation because the signal intensity does not depend linearly on laser intensity. Over the region of a given vibronic progression (~ 200 cm^{-1}), however, the relative spectral intensities are quite accurate.

Based on the spectra, the origin of the diethyl ether-h_{10} spectrum is at 52 675 cm^{-1} and the origin of the diethyl ether-d_{10} spectrum is at 52 926 cm^{-1}. This transition has been assigned previously to the $(n,3s) \leftarrow (2p)^2$ (oxygen) Rydberg transition. The low energy vibrational progression accompanying this transition is not associated with hot bands. The progression is due to a Franck–Condon active

TABLE I. A list of relative transition energies and intensities of the peaks for the low energy progression built on the diethyl ether origin. Exp. indicates the experimental value and Cal. the calculated value. The corresponding diethyl ether-d_{10} results are listed in parentheses.

Vibronic transition	Relative transition energy (cm^{-1})		Relative transition intensity	
	Exp.	Cal.	Exp.	Cal.
$0 \rightarrow 0$	0(0)	0(0)	0.20(0.04)	0.06(0.01)
$0 \rightarrow 1$		0.4(0)		0(0)
$0 \rightarrow 2$	62(56)	64(56)	1.00(0.49)	1.00(0.29)
$0 \rightarrow 3$		75(58)		0(0)
$0 \rightarrow 4$	118(94)	116(94)	0.73(1.00)	0.95(1.00)
$0 \rightarrow 5$		154(113)		0(0)
$0 \rightarrow 6$	200(146)	200(143)	0.16(0.37)	0.22(0.36)
$0 \rightarrow 7$		250(175)		0(0)
$0 \rightarrow 8$	(210)	(212)	(0.09)	0.04(0.08)

mode, as can be seen by comparing the h_{10} and d_{10} vibrational spacings in Fig. 1.

The first three prominent vibronic features following the 0_0^0 transition for diethyl ether-h_{10} are at 62, 118, and 200 cm^{-1} from the origin. Diethyl ether-d_{10} displays four prominent vibronic features near its 0_0^0 transition; these lie to the blue of the origin at 56, 94, 146, and 210 cm^{-1}. This pattern remains for all diethyl ether vibronic transitions; a four member progression is built on the vibronic transitions for diethyl ether-h_{10} and a five member progression is built on the vibronic transitions for diethyl ether-d_{10}. The spacings, isotopic effects, and intensity patterns for these progressions all support the assignment of these features as a progression in a single low energy diethyl ether vibrational motion. Identification of the particular motion involved will be discussed in Sec. IV. Additionally, as will become clear in the ensuing Discussion section, these features (intensities and spacings) can be fit with a single parameter (the ratio of the ether-h_{12} and -d_{12} reduced masses for the mode). All observed and analyzed features are known to be cold bands as indicated in the last section.

Three higher energy modes can be identified in the spectra for diethyl ether-h_{10} (see Fig. 1). These occur at 408, 816, and 1356 cm^{-1}. Based on a straightforward comparison with known ground state vibrations,[11] these modes can be assigned—408 cm^{-1} is the COC bend (a_1, 444 cm^{-1} in S_0); 816 cm^{-1} is the CO stretch (a_1, 848 cm^{-1} in S_0); and 1356 cm^{-1} is the methylene wag (a_1, 1417 cm^{-1} in S_0). The comparable diethyl ether-d_{10} modes are found at 364 cm^{-1} (395 cm^{-1} in S_0), 730 cm^{-1} (698 cm^{-1} in S_0), and 1056 cm^{-1} (1175 cm^{-1} in S_0). The ground state diethyl ether-d_{10} CO stretch assignment is uncertain based on these results. Another possible ground state assignment for this mode is reported at 761 cm^{-1}.[11] Other weak features ($\sim 53\,000$ cm^{-1} for h_{10}) in these spectra may be associated with additional conformers of diethyl ether.

A double well potential with four adjustable parameters is used to fit the spacing of the low energy progressions observed for diethyl ether-h_{10} and diethyl ether-d_{10} simultaneously. The results are listed in Table I. The parameters obtained from fitting the h_{10} experimental data are
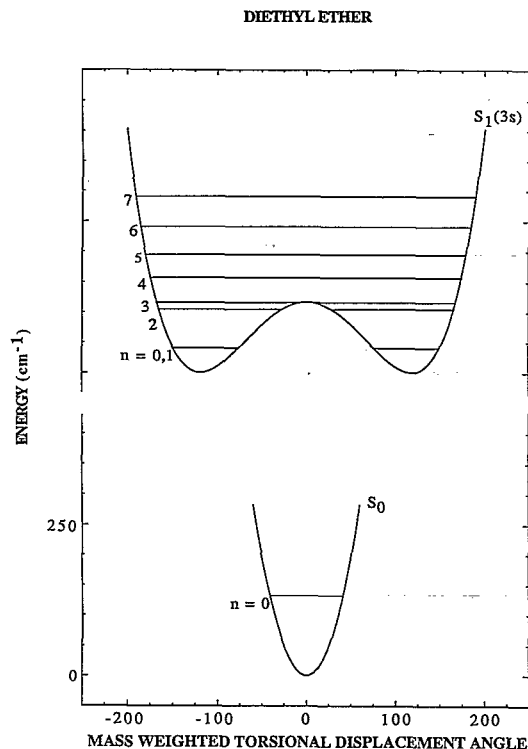
DIETHYL ETHER

FIG. 2. The potential energy curve for diethyl ether as a function of the mass weighted coordinate units. (Bottom) This curve is derived from the experimentally determined ground state (S_0) torsional frequency assuming the motion is harmonic. (Top) This curve is derived from a fit to the low frequency vibrational progression for the transition. The labels near the vibrational energy levels indicate the vibrational quantum number. The vibronic selection rule for the $S_1 \leftarrow S_0$ transition is from the $n=0$ in the S_0 state to $n=0,2,4$,etc. in the S_1 state.

$$\tfrac{1}{4}\hbar\beta = 6.0 \ \mathrm{cm}^{-1},$$

$$\nu_2 = -6.4,$$

$$\nu_4 = 1.05,$$

and

$$\mu_h/\mu_d = 0.60.$$

Substituting these parameters into Eq. (1), the excited state potential for this mode is expressed as

$$V(x) = -0.0167(\sqrt{\mu}x)^2 + 5.96 \times 10^{-7}(\sqrt{\mu}x)^4, \quad (12)$$

in which x is an angular displacement coordinate in degrees, μ is the reduced mass in amu $\mathring{A}^2$, and the numerical constants have units such that V is given in cm^{-1}. $\sqrt{\mu}x$ is referred to as a mass weighted coordinate and is approximately the normal coordinate responsible for the observed progression. To evaluate Eq. (12), this coordinate is approximated as a torsional motion and its reduced mass must be specified. Details of this calculation are discussed in Sec. IV. Figure 2 shows a plot of the potential energy as a function of the mass weighted displacement coordinate based on expression (12). The energy minimum of this function is displaced 118.5 mass weighted coordinate units from the barrier and the barrier height is 117 cm^{-1}.
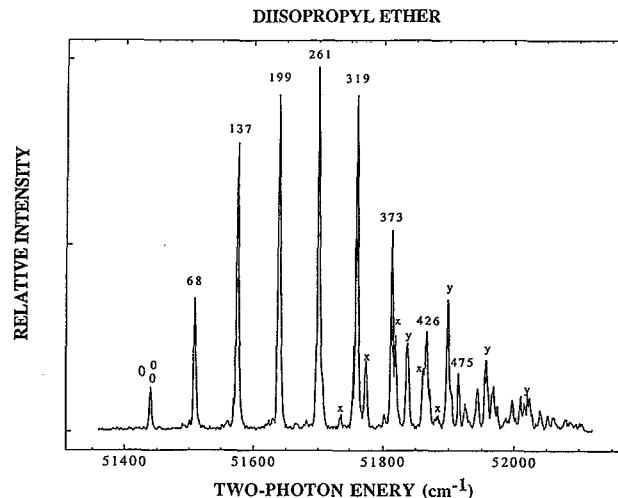
DIISOPROPYL ETHER

FIG. 3. Two photon resonance enhanced multiphoton ionization spectrum of diisopropyl ether. The x axis labels represent the two photon transition energies. The feature labeled 0_0^0 is the spectral origin and the other labels on each feature represent the relative energy with respect to the origin in wave numbers. Two groups of features labeled x or y are independent progressions which probably belong to other ether conformers.

B. Diisopropyl ether

The two photon resonance enhanced MRES of diisopropyl ether, in the region of its $(n,3s)$ origin, is displayed in Fig. 3. The first observed transition falls at 51 440 cm^{-1} and is assigned as the origin of the $(n,3s) \leftarrow (2p)^2$ Rydberg transition.[2] The decrease in transition energy for diisopropyl ether compared to diethyl ether shows the effect of α-carbon methylation on the transition energy.

Up to nine members of the low energy vibrational progression built on the origin can be identified. Note that while this progression is not particularly harmonic ($\Delta v = 5$ is found at 319 rather than 340 cm^{-1}), it is quite regular, suggesting that the double well barrier is not surmounted by up to $v = 9$ in the excited sate. The spacing between peaks in the progression starts at 68 cm^{-1} and monotonically decreases to 49 cm^{-1} for the ninth peak (475 cm^{-1}).

Other modes can be identified in the spectrum of diisopropyl ether (Fig. 3), which also have progressions built on them. These are labeled as x and y and appear in the range 51 700–52 000 cm^{-1}. Progressions in ~65 cm^{-1} can be identified starting at ~51 705 and ending near 52 000 cm^{-1}. At present, these features could be assigned as either due to different vibrational modes of a single conformer or to origins of different conformers.

As for the case of diethyl ether, the first set of progressions is fit to the potential discussed above with three adjustable parameters. The calculated excited state vibrational energies are listed in Table II. The resulting parameters are $\tfrac{1}{4}\hbar\beta = 3.7$ cm^{-1}, $\nu_2 = -11.2$, and $\nu_4 = 0.436$; the standard deviation of the fit is less than 2 cm^{-1}. The potential can be expressed as

$$V(x) = -0.011(\sqrt{\mu}x)^2 + 5.8 \times 10^{-8}(\sqrt{\mu}x)^4. \quad (13)$$

TABLE II. A list of relative transition energies and intensities of the peaks for the low energy progression built on the diisopropyl ether origin.

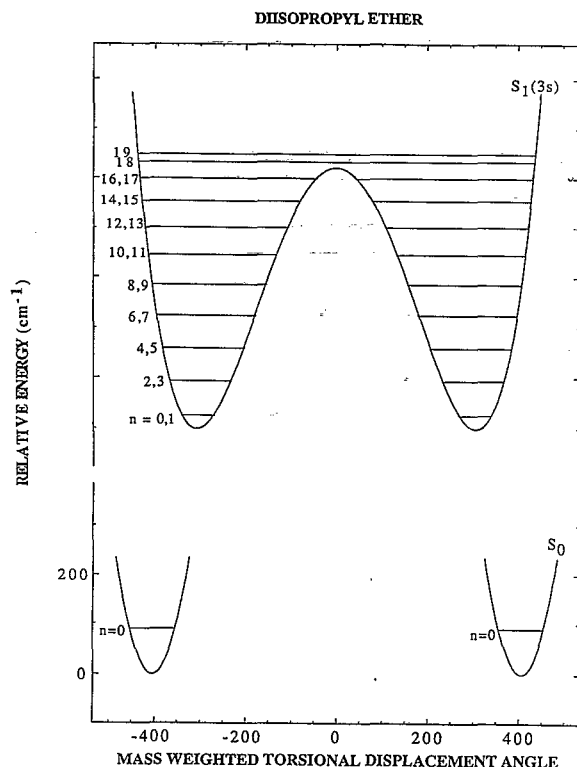| Vibronic transition	Relative transition energy (cm^{-1})		Relative transition intensity	
	Exp.	Cal.	Exp.	Cal.
0→0	0	0.0	0.12	0.17
0→1		0.0		0.00
0→2	68	68.0	0.37	0.52
0→3		68.0		0.00
0→4	137	134.2	0.79	0.85
0→5		134.2		0.00
0→6	199	198.2	0.98	1.00
0→7		198.2		0.00
0→8	261	259.8	1.00	0.95
0→9		259.8		0.00
0→10	319	319.0	0.94	0.78
0→11		319.0		0.00
0→12	373	375.0	0.57	0.59
0→13		375.2		0.00
0→14	426	427.5	0.27	0.42
0→15		427.9		0.00
0→16	475	474.2	0.15	0.23
0→17		475.9		0.00
0→18	504	508.0	0.11	0.18
0→19		524.4		0.00

FIG. 4. The potential energy curve for diisopropyl ether as the function of the mass weighted coordinate units. (Bottom) This curve is derived from the experimentally determined ground state (S_0) torsional frequency assuming the motion is harmonic, and two harmonic wells represent the double well nature. The displacement of the ground state minimum is determined from a fit of the transition intensity distribution. (Top) This curve is derived from a fit to the low frequency vibrational progression for the transition. The labels near the vibrational energy levels indicate their vibrational quantum number.
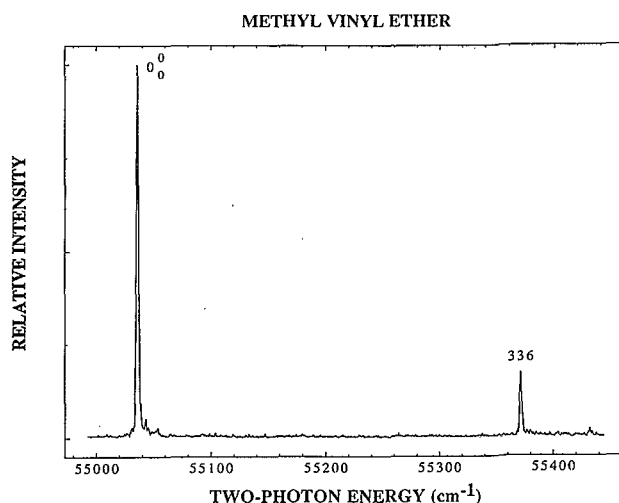
The units of $V(x)$ and $\sqrt{\mu}x$ are the same as in Eq. (12). A plot of Eq. (13) is displayed in Fig. 4. Again, this is a double well potential for the excited state. The barrier for this potential is 521 cm^{-1} and the energy minima are shifted 308 mass weighted coordinate units from the barrier center. Note that every excited state vibration is a doublet below the barrier with less than 1 cm^{-1} splitting (which cannot be distinguished on the scale of this plot). Modes above the barrier begin to have more significant splittings. This is consistent with the experimental observation that the peaks in this progression are single lines within the experimental resolution. Peaks which arise due to transitions to vibrational levels above the barrier can be assigned based on the calculational results. For example, the peak in the spectrum at 504 cm^{-1} (51 945 cm^{-1}) may be assigned as the tenth member of this progression. Without knowing its calculated value of 508 cm^{-1}, this feature would be difficult to assign.

C. Methyl vinyl ether

The two photon resonance MRES of methyl vinyl ether is displayed in Fig. 5. The one photon absorption spectrum of this molecule has not been reported. The first observed peak is at 55 036 cm^{-1}, which is considerably higher than the energy observed for the other ethers studied here. It is assigned as the $(n,3s)$ transition origin. The high transition energy for the molecule can be qualitatively considered to be due to conjugation of the $2p$ lone pair electron with the ethylene π bond. This delocalization of the lone pair would lower the energy of the $2p$ orbital in the ground state, but the $3s$ orbital would not experience this

FIG. 5. The two photon resonance enhanced multiphoton ionization spectrum of methyl vinyl ether. The feature labeled 0_0^0 is the spectral origin. The label 336 represents the relative energy of the peak with respect to the origin in wave numbers.
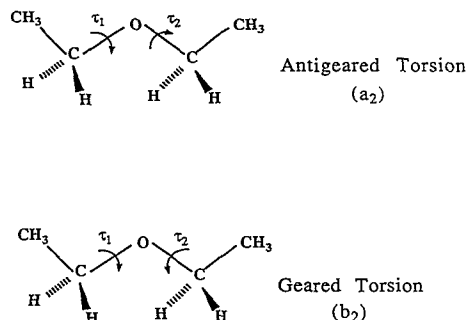
FIG. 6. A schematic diagram of the torsional motion for diethyl ether. The top diagram shows the antigeared torsional motion in which the ether alkyl chains rotate in the opposite direction. The bottom diagram shows the geared motion in which the ether alkyl chains rotate in the same direction.
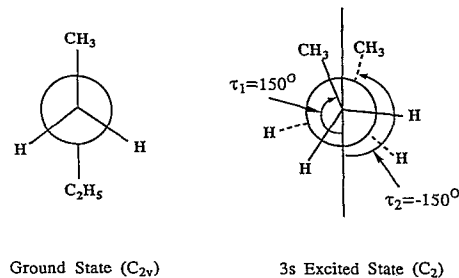

FIG. 7. Newman projection diagrams of ground and excited state diethyl ether. The ground state geometry has been determined experimentally and by a MOPAC6 calculation. The excited state equilibrium configuration is determined by the potential energy minimum shift which is shown in Fig. 2.

stabilization. Valence singlet states, presumably displaying broad absorption, should also exist in this region, but have not been observed.

The observed vibronic structure for methyl vinyl ether is considerably simpler than that of the ethers discussed above. The first observed peak is at 336 cm^{-1}. No other significant features are observed. The observed ground state in-plane (COC) bending mode (a') is reported at 310 cm^{-1} (Ref. 12) and is a possible candidate for the assignment of this feature.

D. Semiempirical calculations

Before considering the calculational results, we should first consider the description of the geometry of diethyl and diisopropyl ethers. The relative conformation of the two halves of these symmetrical molecules is defined by two C-O-C-C dihedral angles τ_1 and τ_2. The planar heavy atom *trans-trans* equilibrium conformation of diethyl ether has τ_1 and τ_2 equal to 180° and −180°, respectively. The diisopropyl ether equilibrium structure can be described by the same two dihedral angles, which are in this instance less than ±180°. The relative motion of the two hydrocarbon moieties of these ethers (torsional vibrations) can be described in terms of τ_1 and τ_2 as well. A geared motion involves both τ_1 and τ_2 decreasing or increasing in phase and an antigeared motion involves τ_1 and τ_2 simultaneously increasing and decreasing out of phase. See Fig. 6 for a pictorial representation of those torsional motions.

The set of MOPAC6 programs,[13] which performs semiempirical molecular orbital calculations, is used to calculate minimum energy ground state geometries, employing the AM1 Hamiltonian. The ground state geometry optimization for diethyl ether predicts that the most stable geometry is planar *trans-trans* (TT, $\tau_1,\tau_2 = \pm 180°$) with C_{2v} symmetry (Fig. 7). This result is consistent with all previous experimental determinations of the ground state structure.[14] The antigeared torsional motion (to be proposed in the Discussion section as responsible for the low energy progression observed for diethyl ether) is illustrated in Fig. 6 along with the geared torsional motion. A potential energy curve for the antigeared torsional coordinate

motion is calculated with MOPAC6 by fixing the molecular geometry along this displacement and optimizing all other degrees of freedom. This calculated potential energy curve is plotted in Fig. 8. The *gauche-gauche* (GG) $\tau_1,\tau_2 = \pm 90°$ geometry is a local minimum as shown in the figure. The experimental energy difference between the TT and GG conformers is reported to be 875 cm^{-1} (Ref. 15); the calculations yield a 350 cm^{-1} energy difference for these conformers. A normal mode analysis (MOPAC6) gives the antigeared torsional motion at 34 cm^{-1}. It is assigned at 130 cm^{-1} based on a solid state Raman experiment.[11]

A similar calculation is also performed for diisopropyl ether. As shown in Fig. 9, the H-C-O-C dihedral angle at minimum energy geometry is calculated to be 37°. The experimentally determined value for the H-C-O-C angle is 39°.[16] The C-C-O-C dihedral angles (τ_1,τ_2) are calculated to be ±155° and equivalently ±85°. A potential energy profile for the antigeared torsional motion of di-
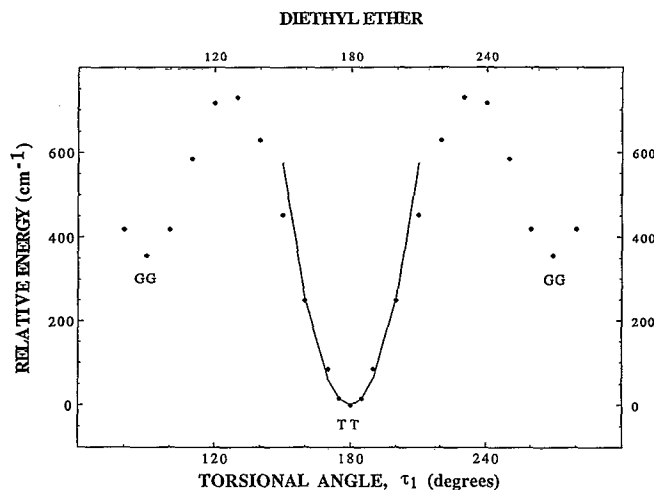

FIG. 8. The potential energy curve for the ground state of diethyl ether along the antigeared torsional coordinate ($\tau_2 = -\tau_1$). Dots represent configuration energies from the MOPAC6 calculation and the solid curve is the best fit to these points with a harmonic oscillator potential function. TT and GG represent *trans-trans* and *gauche-gauche* stable energy geometries.

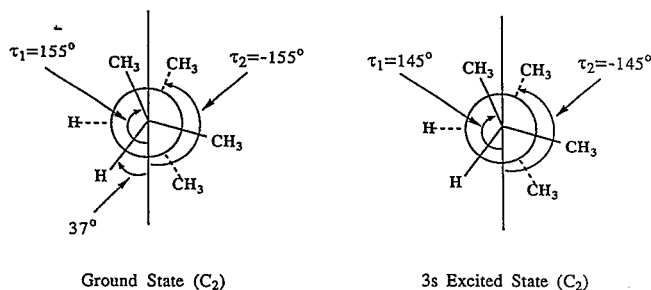Ground State (C₂)   3s Excited State (C₂)

FIG. 9. Newman projection diagrams of the ground and excited states of diisopropyl ether. The ground state geometry has been determined experimentally and by a MOPAC6 calculation. The excited state configuration is determined by the potential energy minimum shift which is shown in Fig. 4.

isopropyl ether similar to that of diethyl ether is shown in Fig. 10. The potential has a double minimum and a barrier height of 500 cm^{-1} at a C–C–O–C dihedral angle of $\pm 120°$.

IV. DISCUSSION

In this section, we will focus on the nature of the vibrational coordinate along which both diethyl and diisopropyl ethers are displaced upon excitation from the ground state to the $(n,3s)$ oxygen Rydberg state. Based on the foregoing discussion, we only know that the excited state potential for the progression forming mode is of a double minimum form as modeled by Eqs. (1), (12), and (13). The appropriate mode can be found through Franck–Condon intensity calculation and an assumed similarity between the diethyl and di-isopropyl ether behavior.

The most interesting feature of both the diethyl and diisopropyl ether spectra is the prominent vibronic progression in a single low energy mode built on all observed
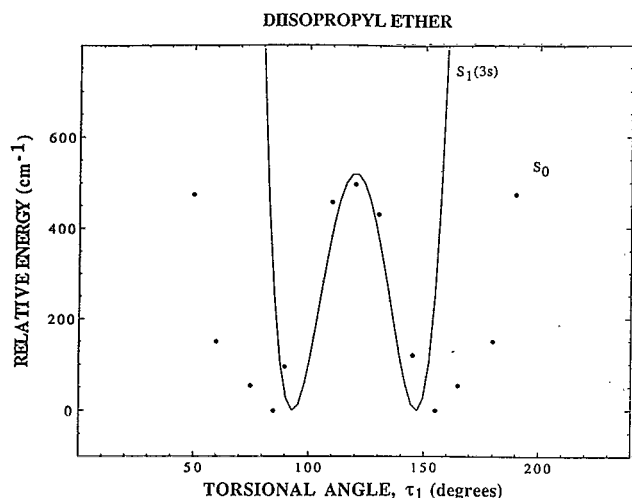

FIG. 10. The potential energy curve for ground and excited states of diisopropyl ether along the antigeared torsional coordinate $(\tau_2 = -\tau_1)$. Dots represent configuration energies from the MOPAC6 calculation and the solid curve is the excited state potential shown in Fig. 4 when projected on the ground state.
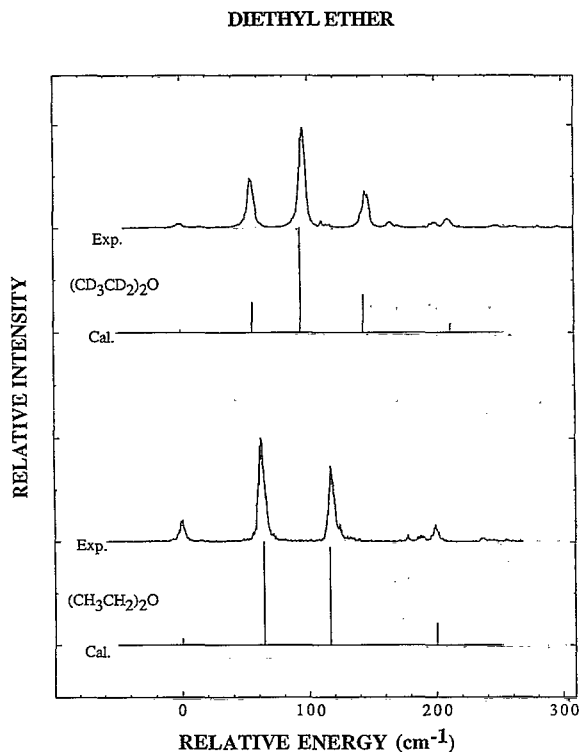
vibronic origins. This progression is similar to that found for ammonia in its first excited $(n,3s)$ Rydberg state; however, no report of comparable behavior for open chain ethers has appeared. The detailed nature of the appropriate normal mode for the excited state distortion of open chain ethers is not obvious.

Three general types of motion can be identified in diethyl ether that can be both of low energy and can reasonably generate a distortion in the excited $(n,3s)$ Rydberg state. These are the C–O–C–C torsions depicted in Fig. 6, two CH_3 torsions (a_2 and b_2), and the totally symmetric C–C–O bend. All other modes have ground state energies well in excess of 400 cm^{-1} and are not considered likely candidates for the progression forming mode observed in the spectra of the two ethers.

Based on the isotope shifts for the diethyl ether system, the methyl torsions can be eliminated as the mode responsible for the observed progressions. Additionally, one would not expect that a Rydberg transition from a nonbonding $(2p)^2$ orbital to a nonbonding $(n,3s)$ orbital would have a large effect on a totally symmetric bending mode. The change in bond character would have to be sufficient to account for a change in vibrational frequency of a factor of 4. We consider this latter possibility unlikely and thus only seriously consider the possible progression forming mode to be one of the C–O–C–C (geared or antigeared) torsional modes.

The observed excited state vibrational spacings for diethyl ether-h_{10} are 62, 56, and 86 cm^{-1}, and for diethyl ether-d_{10} are 56, 38, 52, and 64 cm^{-1}. The uneven spacings are indicative of a double well excited state potential for this molecule,[17] as assigned in the last section. If this progression forming mode is nontotally symmetric in the ground electronic state, the equilibrium geometry of the excited state molecule has a different symmetry than the equilibrium geometry of the ground state. Note that the double well potential is not consistent with the totally symmetric O–C–C bending mode as the progression forming displacement.[18]

The C–O–C–C torsional motion gives rise to two possible double well distortions—the geared (b_2 in the ground state) torsion which preserves the C_2 molecular axis and the excited state surface has C_2 symmetry, and the antigeared (a_2 in the ground state) torsion which preserves the σ_v plane and the excited state surface has C_s symmetry. As discussed by Herzberg, both possibilities result in symmetry allowed vibronic transitions.[18] Thus the excited state potential curve of Fig. 2 can be applied to either torsional mode.

The relative transition intensities for this progression can be calculated based on a ground state torsional mode energy of 132 cm^{-1} and the assumption that the mode is harmonic. The calculated relative intensities for the low energy progression of diethyl ether-h_{10} and -d_{10} are obtained as described in Sec. II B and are presented in Fig. 11. The relationship between the ground and excited state potential surfaces is shown in Fig. 2. No adjustable parameters are employed in the calculation. This agreement supports the choice of the C–O–C–C torsional motion for the

DIETHYL ETHER

FIG. 11. The low frequency Franck–Condon progression built on the diethyl ether origin. Curves represent the experimental data and lines represent the calculated best fit to the experimental data using models discussed in the test.
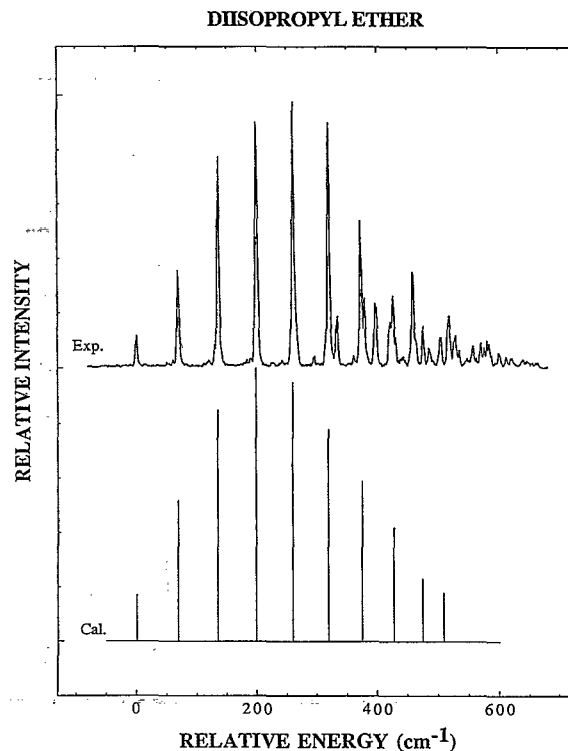
DIISOPROPYL ETHER

FIG. 12. The low energy Franck–Condon progression built on the di-isopropyl ether origin. Curves represent the experimental data and lines represent the calculated fit to the experimental data using the model discussed in the test assuming C–O–C–C antigeared torsional motion responsible for the progression.

low frequency mode, but still cannot by itself distinguish between the geared and antigeared motion represented in Fig. 6.

The diisopropyl ethyl spectrum can be used to distinguish between the two possible choices for diethyl ether torsional vibrational motion if the two cases are assumed to be comparable and the same torsional mode is assumed responsible for the displacement. The observed progression in the diisopropyl ether spectrum is even more extensive than that characterized for diethyl ether. The analogous torsional motion of the ground electronic state of diisopropyl ether is determined to be 90 cm^{-1}.[18] The equilibrium C_2 ground state geometry for diisopropyl ether is depicted in Fig. 9. The geometries of the two ethers are similar except that the ground state equilibrium C–C–O–C dihedral angles (τ_1,τ_2) are $\pm85°$ or $\pm155°$ for diisopropyl ether[16] and $\pm180°$ for the diethyl ether. MOPAC6 calculations give the two minima at $\pm155°$ and $\pm85°$ with the maximum in the potential at $\pm120°$. The barrier between the two minima at $\pm155°$ and $\pm85°$ is 500 cm^{-1} at $\pm120°$.

Both geared and antigeared torsional motions (involving τ_1 and τ_2) exist for diisopropyl ether. The geared, nontotally symmetric (b) motion in the ground state gives rise to a single minimum potential curve centered at the equilibrium conformation of the ground state. The antigeared totally symmetric (a) motion in the ground state must give rise to a double well potential curve with the two minima

at the equilibrium geometry of the ground state $(\tau_1,\tau_2 = \pm155°$ or $\pm85°)$.

The experimental progression in the low energy mode requires a double minimum well in the excited state based on the observed excited state vibrational energies. We can employ the two model potential curves based on the two possible torsional motions to calculate the relative intensities of the members of this progression. These intensities cannot be reproduced using the geared torsional motion with a single well ground state potential and the observed excited and ground state energies. The antigeared torsional motion, on the other hand, gives an excellent fit to both the progression energies and intensities (Table II and Fig. 12). The calculations are performed under the assumption that the antigeared ground state torsion is harmonic (90 cm^{-1}). The fit is generated with the position of the ground state well relative to the barrier of excited state potential as the only parameter, $\sqrt{\mu}x_{min} = 405$ amu Å^2 for the ground state. Since the barrier is so large for the ground state, the transitions can be considered to originate at the zero point energy of a single displaced well. A comparison between the two electronic state wells is given in Fig. 10. The wells differ in shape, barrier height, and position of the minima. The shift in the position of the minima is mainly responsible for the observed progression.

This model predicts correctly that the excited state barrier for di-isopropyl ether is much larger than that for

diethyl ether. The large barrier for diisopropyl ether is caused by steric interactions present in this molecule in the ground state and is not directly related to the Rydberg state. In the $(n,3s)$ Rydberg state, the double minimum will become narrower and the structure becomes less ideally TT (dihedral angle of 180°). This is depicted in Figs. 9 and 10.

We conclude based on these results that the active progression forming mode for diisopropyl ether is the antigeared totally symmetric C–O–C–C torsion. Given this conclusion, we suggest that the same torsional motion (see Fig. 6) is responsible for the progression in diethyl ether.

Simulation of the experimental results with a potential of an assumed functionality yields a curve in mass weighted coordinates. In order to make a direct comparison to a calculated potential function based on a particular normal coordinate, one must know the reduced mass of the chosen normal mode. In the ensuing discussion, we assume that the reduced mass of the ground and excited state normal modes is the same. One can estimate the reduced mass of the normal mode of interest in two ways.

First, assume that the ground state potential for diethyl ether along the antigeared torsional coordinate, as determined by the MOPAC6 calculation, is harmonic near the energy minimum. Then

$$V(x) = 0.0786(\sqrt{\mu}x)^2. \tag{14}$$

The harmonic energy of this mode is taken to be the experimentally determined value of 132 cm^{-1}.[11] A least squares fit can be carried out with the reduced mass μ as the only variable. The resulting reduced mass is 8 amu Å^2 for diethyl ether.

Second, assume the antigeared torsion is not coupled to any other motion and is responsible for the progression. The calculated reciprocal mass matrix G should then yield the reduced mass of this mode. Following the method described by Decius,[19] the calculated reduced mass is 25 amu Å^2 for the pure antigeared torsional mode for diethyl ether.

The reduced mass value resulting from fitting the calculated potential to a harmonic oscillator probably represents a lower bound to the actual coordinate reduced mass because the MOPAC6 normal mode analysis energy for this mode is 34 cm^{-1} rather than the assigned 132 cm^{-1}.[11] Additionally, the calculated TT and GG conformer energy separation is a factor of 2 too small. Making the calculated surface steeper to match the experimental results will increase the reduced mass by a factor of 2 to 3.

If we somewhat arbitrarily take the reduced mass for this mode to be 25 amu Å^2 based on the G matrix element calculation and employ the relation

$$\sqrt{\mu}x_{min} = 118.5 \text{ amu Å}^2$$

based on Eq. (12) and the discussion following it in Sec. III, a displacement angle for diethyl ether of 23° results. The excited state is distorted from planarity and the C–O–C–C dihedral angle is 157°. If the mode reduced mass is increased or decreased by a factor of 2 (12–50 amu Å^2),

the dihedral angle ranges from 164° to 147°, but the physical picture of the motion and distortion remains the same.

A similar treatment can be applied to the diisopropyl ether system for which the reduced mass of the torsional mode is also unknown. A calculation of the G matrix element for this mode, as performed above, yields the same value as obtained for the comparable mode of diethyl ether (25 amu Å^2). Additionally, one can use the existing experimental data to determine a value for the excited state displacement.

Assuming that the diisopropyl ether ground state well is harmonic near the minimum, we obtain for this well a value of $\sqrt{\mu}x_{min} = 405$ amu Å^2 from a calculation of the intensity of the progression in the torsional mode. The MOPAC6 ground state geometry and the electron diffraction results[16] yield the potential minimum displacement from the barrier position (120°) as $x = 35°$. The reduced mass values for the ground state torsion then becomes 134 amu Å^2. Based on this reduced mass, the excited state minimum is calculated to be displaced from the barrier by 26°. The dihedral angle of the minimum energy configuration in the excited state is 146° for diisopropyl ether (Fig. 9). The ground state dihedral angle for diisopropyl ether is 155°. This ~10° shift gives rise to the extensive progression observed in the spectrum. These exact values of course also depend on the assumption that the reduced mass for the antigeared torsional mode is the same in both ground and excited states.

No progressions are observed for methyl vinyl ether. The ground state of this molecule has two accessible geometries—one has the methyl group *syn* with respect to the vinyl group and the other has the methyl group *anti* with respect to the vinyl group. The *syn* geometry is reported to be more stable.[12] The torsional motion about the O–CH bond of the vinyl moiety must be hindered by the delocalization of the $2p$ oxygen electrons over the π system. Nevertheless, the methyl group could still undergo rotation (perhaps hindered) about the O–CH$_3$ bond. The absence of progressions in the methyl vinyl ether spectrum implies that the $3s \leftrightarrows 2p$ Rydberg excitation does not influence the potential for rotation at the α carbon. The prominent progressions found for the other two ethers must reflect the change in potential at the β-carbon position. The change in potential must occur through nonbonded interactions. This suggests that the $3s$ and $2p$ electrons have significantly different distributions in the molecule.

V. CONCLUSIONS

We have obtained two photon resonance enhanced MRES of supersonic expansion cooled diethyl ether-h_{10}, and -d_{10}, diisopropyl ether, and methyl vinyl ether. This technique achieves high resolution spectra of the $2p3s \leftarrow (2p)^2$ oxygen Rydberg transition in these molecules. The spectra show significant progressions in a low energy vibrational mode in both diethyl and diisopropyl ethers, but not in methyl vinyl ether. The progression forming mode can be assigned as the antigeared torsional mode associated with a C–O–C–C *dihedral angle displacement*

upon electronic excitation. A double well potential function is employed to model the excited state progressions with only three adjustable parameters. The transition intensities for the progressions in diethyl and diisopropyl ethers are calculated based on MOPAC6 and experimental studies of the ground state surfaces. Intensity calculations for the diisopropyl ether Rydberg state progression correctly identify the progression forming mode as the antigeared torsion of the C–O–C–C dihedral angle. The progression forming mode in diethyl ether is assigned to be the same one.

The torsional displacement active in the $2p3s \leftarrow (2p)^2$ oxygen Rydberg transition is suggested to arise from the interaction between the $3s$ electron and the β-methyl groups on both diethyl and diisopropyl ethers. This nonbonded interaction probably reflects the diffuse nature of the $3s$ molecular Rydberg orbital.

ACKNOWLEDGMENT

[1] M. Robin, *Higher Excited States of Polyatomic Molecules* (Academic, New York, 1974), Vol. 1.

[2] W. R. Harshbarger, J. Chem. Phys. **53**, 903 (1970).

[3] T. J. Cornish, T. Baer, and L. G. Pedersen, J. Phys. Chem. **93**, 6064 (1989).

[4] P. O. Moreno, Q. Y. Shang, and E. R. Bernstein, J. Chem. Phys. **97**, 2869 (1992).

[5] W. R. Wadt and W. A. Goddard III, Chem. Phys. **18**, 1 (1976).

[6] J. A. Horsley and F. Flouquet, Chem. Phys. Lett. **5**, 165 (1970).

[7] J. A. Horsley and W. H. Fink, J. Chem. Phys. **50**, 750 (1969).

[8] L. J. Bremner, M. G. Curtis, and I. C. Walker, J. Chem. Soc. Faraday Trans. **87**, 1049 (1991).

[9] R. McDiarmid, J. Chem. Phys. **60**, 3340 (1974).

[10] R. L. Somorjai and D. F. Hornig, J. Chem. Phys. **36**, 1980 (1962).

[11] J. R. Durig and J. S. Church, Mol. Cryst. Liq. Cryst. **69**, 217 (1981).

[12] P. Cahill, L. P. Gold, and N. L. Owen, J. Chem. Phys. **48**, 1620 (1968).

[13] J. J. P. Steward, a general molecular orbital package (MOPAC), 6th ed., 1989.

[14] M. Hayashi and K. Kuwada, Bull. Chem. Soc. Jpn. **47**, 3006 (1974).

[15] J. P. Perchard, J. C. Monier, and P. Diazabo, Spectrochim. Acta Part A **27**, 447 (1971).

[16] H. Takeuchi, M. Fujii, S. Konaka, and M. Kimura, J. Phys. Chem. **91**, 1015 (1987).

[17] D. G. Lister, J. N. Macdonald, and N. L. Owen, *Internal Rotation and Inversion* (Academic, New York, 1978).

[18] G. Herzberg, *Electronic Spectra of Polyatomic Molecules* (Van Nostrand Reinhold, Princeton, NJ, 1966).

[19] J. C. Decius, J. Chem. Phys. **16**, 1025 (1948).